IOSR Journal of Computer Engineering (IOSR-JCE)
e-ISSN: 2278-0661,p-ISSN: 2278-8727, Volume 24, Issue 2, Ser. IV (Mar. –Apr. 2022), PP 39-59
www.iosrjournals.org

Power consumption reduction on RADAR MIMO using Lift Wavelet Transform – Universal Filtered Multicarrier (LWT-UFMC)

Marie Emile RANDRIANANDRASANA[1], Paul Auguste RANDRIAMITANTSOA[2], Andry Auguste RANDRIAMITANTSOA[2]
[1](Department of Telecommunication, Antsirabe Vankinankaratra High Education Institute, Antsirabe)
[2](Department of Telecommunication, High School Polytechnic of Antananarivo, Anosizato)
[3](Department of Telecommunication, High School Polytechnic of Antananarivo, Anosizato)

Abstract:
Background*: The RADAR MIMO uses multiple antennas on emitter and receiver for avoiding doppler effects, improving the robustness of binary error of transmission. Multi carrier modulation is introduced to have good performance about doppler effects like Universal Filtered Multicarrier (UFMC) used specially on 5G. This modulation is like Orthogonal Frequency Division Multiplex (OFDM) but divides into multiple sub-bands. The problem of OFDM and UFMC is concerned about Discret Fourier Transform (DFT) which gives Peak Average Power Ratio (PAPR) and high time processing. This article replaces the DFT by Discret Cosine Transform (DCT) and Lift Wavelet Transform (LWT). I also noticed that the LWT-UFMC is a proposition on 6G modulations and FFT is the same function as DFT. The difference is that FFT uses rapid multiplication instead of simple multiplication.*
Materials and Methods*: This study presents the difference between RADAR MIMO OFDM and RADAR MIMO UFMC. We did a simulation on Matlab about the RADAR MIMO UFMC using multiple transformations like DFT, DCT and LWT and compared the results (Power Average Power Ration or PAPR, Bit Error Ratio or BER) on each methods. We present all mathematics formulas with simplified diagrams and evaluate the time complexity of each method.*
Results*: As a result, we can deduce that time consumption for LWT is much lower than DCT and DFT. This method doesn't use exponential calculations but just addition and substraction formula. The LWT also presents a lower PAPR but has a larger BER. So, LWT-UFMC presents a good performance in reduction of power consumption on RADAR MIMO instead of classic DCT or DFT UFMC.*
Key Word*: RADAR; MIMO; LWT; UFMC; PAPR.*

Date of Submission: 14-04-2022 Date of Acceptance: 30-04-2022

I. Introduction

Let's a MIMO radar system colocate N_t emitter antenna and N_r receiver antenna. Let $S_m \in \mathbb{C}^L$, the wave on discret time which should be transmitted. Let $S = [s_1, s_2, \dots, s_{N_t}]^T \in \mathbb{C}^{N_t \times L}$, the matrix of emitter waves where L will be the wavelength. Knowing that, the radar emits M impulsions in the interval of coherent treatment with the frequency f_r.

Target

The target catches signal coming to the emitter and sends this signal. The signal could be expressed by the equation (1) :

$$Y_{t,m} = \beta_t . exp^{j(m-1)\omega_t} a_r(\theta_t) a_t^T(\theta_t) s \quad (1)$$

Where,

$a_t(\theta_t) = [\,1, \dots\,,\ e^{j(N_t-1)\pi d_t sin\theta_t}]^T$: the vector director of the antenna emitter

$a_r(\theta_t) = [\,1, \dots\,,\ e^{j(N_r-1)\pi d_r sin\theta_t}]^T$: the vector director of the antenna receiver.

θ_t : the target's direction of arrival

β_t : the signal's amplitude

$\omega_t = 2\pi f_t, f_t$: the doppler frequency of a normalized target.

First model of received signal
The MIMO radar will be composed by n_T emitter antenna and N_r receiver antenna.

A series of independent signals are transmitted in a logical manner by each transmitting element. Propagation of a signal from a transmitting element to a receiving element results in propagation through a channel with three (03) components:

- a channel of the propagation to the target
- a reflective target
- a channel reverses to the receiving probe.

The two channels will be jointly parameterized by a parametric model, from the parameter **ɤ.**
The target is considered to be specific, in other words, the physical dimensions of the target are rather small, which only turns out to be a point with the eyes of the radar. However, it is possible to consider the target as consisting of several reflecting centers.
For each transmit/receive transmission chain pair, the target response is approximated with a value to follow a random process. The equation (2) is a received signal model, due to a series of transmitted waveforms, a point target of the response vector a and a parametric channel model of ɤ.

$$y = \begin{bmatrix} S(\gamma,1) & 0\cdots & 0 \\ 0 & S(\gamma,2) & \vdots \\ \vdots & \cdots & \vdots \\ 0 & 0\cdots & S(\gamma,n_R) \end{bmatrix} \begin{bmatrix} a_1 \\ a_2 \\ \vdots \\ a_{n_R} \end{bmatrix} + \begin{bmatrix} n_1 \\ n_2 \\ \vdots \\ n_{n_R} \end{bmatrix} \quad (2)$$

Let $e_k(t)$ the respective impulse response of *k* different target.

$$e_k(t) = \sum_{r_f=1}^{R_f} m_{r_f}^{(k)} \delta\left(t - \tau_{r_f}^{(k)}\right) \quad (3)$$

Where,

$m_{r_f}^{(k)}$ and $\tau_{r_f}^{(k)}$: the magnitudes of the response for each repair center r_f and the time delay.

The transmitted waveforms $o_i(t)$ are also normalized to unity energy with energy levels defined by p_i for all $i \in [1,\cdots,T]$. Each waveform is multiplied by a beamforming vector $u_i \in \mathbb{C}^{N_T X1}$ to focus on the transmitted waveforms on the radar scene.

Thus, the transmitted radar MIMO signal represents a linear combination of the totality of all beams of the transmitted and associated waves at similar energy levels. It will be expressed by the equation (4).

$$o(t) = \sum_{i=1}^{T} u_i s_i \sqrt{p_i} \quad (4)$$

Losses or pathloss in free space are expressed by $l_T^{(k)}$ and $l_R^{(k)}$ for transmitting and receiving paths relating to each k individual target of the respective radar. Since each target is at the azimuth angle $\mathfrak{h}_K$ relative to the transmission row, the reflected signal of the k-th target can be defined as :

$$y_k(t) = e_k(t) * \left[\beta_T^H(\mathfrak{h}_k) o(t) l_T^{(k)}\right], k = 1, \ldots, K, \quad (5)$$

Where,

$\beta_T(\mathfrak{h}_K) \in \mathbb{C}^{N_T X1}$: vector of various ranges in the direction of the target

(*) : the convolution operator

$(.)^H$: Hermitian or the complex transpose operator

When the reflected signal is received by the RADAR MIMO receiver, the received signal is expressed as the equation (6) :

$$z_r(t) = \sum_{k=1}^{K}\sum_{i=1}^{T} \alpha_{ri}^{(k)}[e_k(t) * o_i(t)]\sqrt{p_i} + \sum_{e=1}^{C_s}\sum_{i=1}^{T} \mu_{ri}^{(e)}\,[e_e(t) * o_i(t)]\sqrt{p_i} + v_r^H \eta(t) \quad (6)$$

Where,

$\beta_R(\theta_k) \in \mathbb{C}^{N_R X1}$: the vector director of various ranges of reception antenna of the azimuth direction

$\theta_k, \alpha_{ri}^{(k)} = l_R^{(k)} v_r^H \beta_R(\theta_k)\beta_T^H(\mathfrak{h}_k) y_k l_T^{(k)}$: reflexion coefficient

$e = 1, \dots, c_s$: source of clutter

The coefficients of periodic reflection and complexes of "clutter" $\mu_{ri}^{(e)}$ is defined by $\alpha_{ri}^{(k)}$ for the target radar with $\mu_{ri}^{(e)} = \tilde{l}_R^{(k)} v_r^H \tilde{\beta}_R(\tilde{\theta}_e)\beta_T^H(\tilde{\mathfrak{h}}_e) y_k \tilde{l}_T^{(k)}$.

Note that, $\mu_{ri}^{(e)}, \tilde{l}_R^{(k)}$ and $\tilde{l}_T^{(k)}$ define the pathloss coefficients corresponding to each source and "clutter" for the transmission and receiving paths, respectively.

The coefficient $\tilde{\mathfrak{h}}_e$ and $\tilde{\theta}_e$indicates the azimuths at which each source of "clutter" is produced relative to the transmission and receiving ranges, respectively.

Second model of received signal

In this second theory, Uniform Linear Antenna (ULA) uses a vector director to beam the signal in a specific direction. The signal to be transmitted is defined by the equation (7) :

$$x(m) = [x_1(m)\ x_2(m) \dots . x_{n_T}(m)] \quad (7)$$

$x_n(m)$: the bandbase signal of the m-ith emission element at the time index m.

The target with (his emplacement θ_k) receives the signal expressed by :

$$r_k(m) = \sum_{n=1}^{n_T} e^{-j(n-1)\pi sin\theta_k}\, x_n(m), with, k = 1,2, \dots K \quad (8)$$

$$r_k(m) = a^H(\theta_k)x(m) \quad (9)$$

Where : $a(\theta_k)$ is the vector director defined by :

$$a(\theta_k) = [\,1 \quad e^{j\pi sin\theta_k} \quad e^{j2\pi sin\theta_k} \dots \dots . . e^{j(n_T-1)\pi sin\theta_k}] \quad (10)$$

II. Material And Methods

Advanced Muti-carrier modulation

In OFDM the entire bandwidth is divided into a number of sub-carriers and these sub-carriers are transmitted in parallel to increase symbol duration to achieve high data rates; it is shown in figure no 1. An OFDM signal is the sum of all sub-carriers signal which are modulated at the sub channels of equal bandwidth.

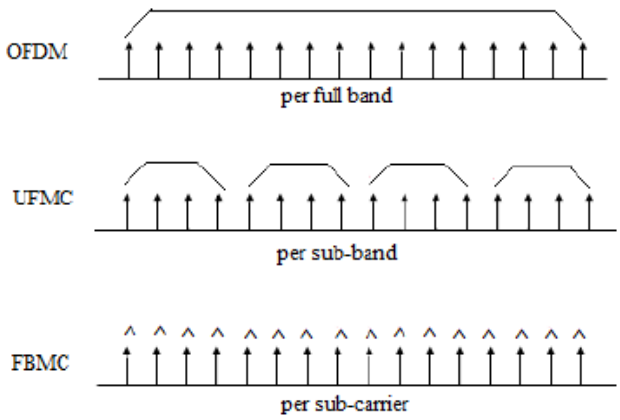

Figure no 1 : Filtering methods in OFDM, UFMC and FBMC

To reduce Out of Band (OOB) on spectrum, advanced new filter give other advanced modulations like Universal Filtered Multicarrier (UFMC) and Filter Bank based MultiCarrier (FBMC).

Offset of Quadrature Amplitude Modulation (OQAM) on advanced modulation
The techniques of OQAM is based on two principles :

- On the emitter, the OQAM preprocessing
- On the receiver, the OQAM postprocessing

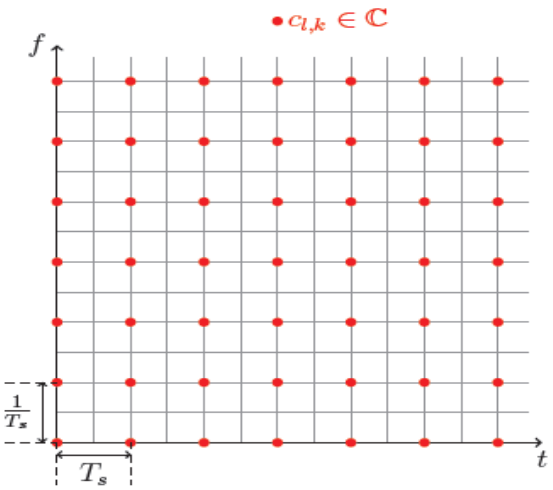

Figure no 2 : Time latency with QAM

The first operation in the pre-processing block is the complex/real conversion. Indeed, instead of sending complex symbols (QAM symbols).
The figure no 2 and 3 show the difference between time latency using QAM processing and OQAM processing with advanced modulation. The constant k and l represent the temporal index and the frequency index, respectively.

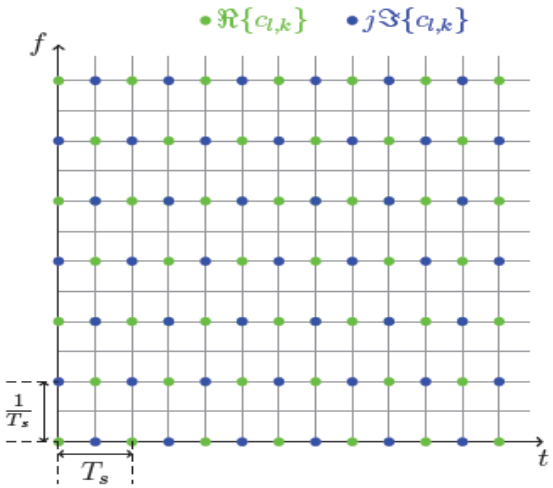

Figure no 3 : Time latency with O-QAM

The objectives of OQAM are:

- Two symbols on the same carrier must be successively real and purely imaginary.
- In addition, the adjacent symbols between the two under carrier must also be successively real and purely imaginary.

Let $C_{l,k}$ the complex symbols that after OQAM modulation will become real symbols $a_{l,k}$ expressed by the equation (11). Recall that k is the temporal index and the frequent index.

$$\boldsymbol{a_{l,k}} = \begin{cases} \boldsymbol{Real(C_{l,k})\ si\ l\ \ pair\ et\ k\ pair} \\ \boldsymbol{Imag(C_{l,k})\ si\ l\ impair\ et\ k\ pair} \\ \boldsymbol{Imag(C_{l,k})\ si\ l\ pair\ et\ k\ impair} \\ \boldsymbol{Real(C_{l,k})\ si\ l\ \ impair\ et\ k\ impair} \end{cases} \tag{11}$$

The second operation of the OQAM pre-processing block is a multiplication by:

$$\theta_{l,k} = j^{l+k}.$$

The symbols at the exit of the OQAM pre-processing block will modulate the carrie and which notes $X_{l,k}$ like on expression :

$$\boldsymbol{X_{l,k}(t)} = \sum_{\boldsymbol{k=-\infty}}^{+\infty} \boldsymbol{\theta_{l,k}.a_{l,k}.\delta(t - k\frac{T_s}{2})} \tag{12}$$

Where,

$\delta(t)$: impulsion of Dirac

The first operation of the OQAM post-processing block is multiplication by $\theta^*_{l,k}$ which is a conjugate complex of $\theta_{l,k}$. Then, there is a real/complex conversion. Indeed, two real symbols successively on a carrier form a complex symbol. The equation (13) gives the expression of complex symbols on the carrier l after OQAM post-processing.

$$\boldsymbol{C_{l,k}} = \begin{cases} \boldsymbol{a_{l,k} + a_{l,k+1}\ \ si\ l\ pair\ et\ k\ pair} \\ \boldsymbol{a_{l,k+1} + a_{l,k}\ si\ l\ impair\ et\ k\ pair} \\ \boldsymbol{a_{l,k-1} + a_{l,k}\ \ si\ l\ pair\ et\ k\ impair} \\ \boldsymbol{a_{l,k} + a_{l,k-1}\ \ si\ l\ impair\ et\ k\ impair} \end{cases} \tag{13}$$

OFDM-OQAM MIMO radar

In MIMO radar system with M transmitter antennas and N receiver antennas, the transmitters are placed parallel to the axis of the abscesses are its antennas are spaced a distance dt, as the coordination of the same meter antenna is expressed by the equation (14).

$$E_m = E_0 + m.d_t.x. \tag{14}$$

Where, m= 0,… ,M-1 and $E_0 = \left[x_{t,0}, y_{t,0}, z_{t,0}\right]^T$

the first transmitter is located in the center O(0,0,0) and et $x = [1,0,0]^T$ is the unitary vector on the axis of x. Similar, the receivers are parallel to the order axis, they are spaced a distance d_r, n-ith receiver antenna are located on coordinate by the equation (15) :

$$R_n = R_0 + n.d_r.y, \tag{15}$$

Where, $R_0 = \left[x_{r,0}, y_{r,0}, z_{r,0}\right]^T$ and $y = [0,1,0]^T$

Each element in a transmitter system transmits a signal modulated in OFDM at an initial carrier frequency f_0. The base band OFDM signal consists of N sub-carrier frequencies with a uniformly spaced frequency Δf; the total bandwidth is expressed by the equation (16).

$$B\omega = N.\Delta f \tag{16}$$

The n-ith sub-carrier is modulated with a K-ith code sequence and it will be formulated by the equation (17) and the code should respect the orthogonal waveform condition :

$$c_{n,p} = \left[b_{n,p}^{(0)}, \dots, b_{n,p}^{(K-1)}\right]^T \tag{17}$$

Where, $c_{n,p}^H c_{n,p} = \begin{cases} 1, & p = p' \\ 0, & p \neq p' \end{cases}$

So, $c_n = \left[c_{n,0}, \dots, c_{n,P-1}\right] \in \mathbb{C}^{K \times P}$ and the expression could be rewrited like :

$$c_n^H c_n = I_n$$

The bit length t_b respects the orthogonality condition $t_b.\Delta f = 1$. The m-ith impulsion on the baseband OFDM could be expressed by the equation (18).

$$u_m(t) = \sum_{n=0}^{N-1} \sum_{k=0}^{K-1} b_{n,m}^{(k)} exp^{\{j2\pi t\Delta f(t-(k+1))t_c\}} rect\left(\frac{t - kt_s}{t_s} - \frac{1}{2}\right) \tag{18}$$

With,

$t_s = t_b - t_c$: symbol duration

$t_c = \propto t_b$: cyclic prefix duration

m = 0,…,P-1

$rect(t) = \begin{cases} 1, & \frac{-1}{2} \leq t < \frac{1}{2} \\ 0, & ailleurs \end{cases}$: rectangular signal

The baseband signal $u_m(t)$ is modulated with an initial carrier frequency f_0 for transmitting.

A target set is composed of the scattered ideal points I. The coordinate of i-th dispersed point is expressed by :

$$D_i = [x_i, y_i, z_t]^T \tag{19}$$

The amplitude of the relative dispersion is σ_i, which is a constant within an OFDM pulse width and for multiple transmitter/receiver channels.

The target velocity is fully estimated and compensated after pre-processing. The Doppler effect is negligible in all echo models as expressed by the equation (20):

$$t = \tau_{min} + kt_s + t_c + t_0, \tag{20}$$

With,

τ_{min} : being the beginning of a sample

$t_0 \in [0, t_b]$: initial time

The time interval of a (p,q)-th transmit/receive chain and i-th scatter is expressed by the equation (21).

$$\tau_{p,q}^{(i)} = \frac{\left(\left\|D_i - t_p\right\| + \left\|R_q - S_i\right\|\right)}{C} - \tau_{min}$$

(21)

Where,
c : the speed of light
The echo after the downlink is expressed by the equation (22).

$$s_q^{(k)}(t_0) = \sum_{p=0}^{P-1}\sum_{i=1}^{I}\sigma_i exp^{(-j2\pi f_0 \tau_{p,q}^{(i)}} \sum_{n=0}^{N-1} exp^{\{i2\pi\Delta f(t_0-\tau_{p,q}^{(i)}\}} \sum_{k'=0}^{K-1} b_{n,p}^{(k')} \\ rect\left(\frac{(k-k')t_s + t_c + t_0 - \tau_{p,q}^{(i)}}{t_s} - \frac{1}{2}\right) + \vartheta_q^{(k)}(t_0) \tag{22}$$

Where,
$\vartheta_q^{(k)}(t_0)$: the noise
and $rect\left(\frac{(k-k')t_s+t_c+t_0-\tau_{p,q}^{(i)}}{t_s} - \frac{1}{2}\right) = \delta(k-k')$; $\delta(.)$ is an impulse function.

For the following, the processing methods will be described.
For q-th element received, and for k-th OFDM bit, the DFT calculation follows the sample index at a fast time. The echo in a frequency domain is written by the equation (23).

$$x_{n,q}^{(k)} = \frac{1}{N}\sum_{n=0}^{N-1} exp^{\left(j2\pi\frac{nl}{N}\right)} s_{lq}^{(k)} = \sum_{i=0}^{I}\sigma_i exp^{\{-j2\pi(n\Delta f+f_0)\tau_{p,q}^{(i)}\}} \sum_{p=0}^{P-1} b_{n,p}^{(k)} + V_{lq}^{(k)} \tag{23}$$

Where,
$x_{n,q}^{(k)}$: the n-th point results of the DFT and the echo in a frequency domain with n-th subcarrier
$V_{lq}^{(k)}$: the noise
N sub-carriers are separated without inter-carrier interference but the echoes received in P transmitting antennas are multiplexed and named serial to parallel.

To separate the transmitter and decode the sub-carriers, each sub-carrier is indexed n, we stack the DFT results of the K bits in a column vector :

$$s_{n,q} = \left[S_{n,q}^{(0)}, \dots, S_{n,q}^{(K-1)}\right]^T \tag{24}$$

Let,

$$s_{n,q} = C_n E_{n,q}\sigma + v_{n,q} \in \mathbb{C}^{K\times 1} \tag{25}$$

Where,

$C_n \in \mathbb{C}^{K\times P}$ and $E_{n,q}$: complex matrix with dimension $P \times I$

$\varepsilon_{n,p,q}^{(i)} = exp^{\{-j2\pi(n\Delta f+f_0)\tau_{p,q}^{(i)}\}}$: element of matrix C_n and the response of i-th disperser to n-th subcarrier for (p,q)-the transmitter/receiver chain.

$\sigma = [\sigma_1, \dots, \sigma_i]^T$: dispersion coefficient

$v_{n,q} = \left[V_{n,q}^{(0)}, \dots, V_{n,q}^{(K-1)}\right]^T \in \mathbb{C}^{K\times 1}$: vector noise

Let,

$$R_{n,,q} = \left[r_{n,0,q}, \ldots, r_{n,P-1,q}\right]^T \in \mathbb{C}^{K\times 1} \tag{26}$$

$$R_{n,q} = C_n^H x_{n,q} = E_{n,q}\sigma + v'_{n,q} \tag{27}$$

Where,

$r_{n,p,,q}$: modulated echo
$v'_{n,q}$: the noise vectors modified without power change

For each OFDM subcarrier, each transmitter/receiver pair :

$$\varepsilon_{n,p,q}^{(0)} = exp^{\{j2\pi(n\Delta f+f_0)\tau_{p,q}^{(0)}\}},$$
$$\tau_{p,q}^{(0)} = \frac{\|o - Z_p\|\|W_q - o\|}{C} - \tau_{min} \tag{28}$$

$r_{n,p,q}$ is multiplied by $\varepsilon_{n,p,q}^{(0)}$ for a compensated initial phase

$$h_{n,p,q} = \varepsilon_{n,p,q}^{(0)} r_{n,p,q} = \sum_{i=1}^{I} exp^{\{j2\pi(n\Delta f+f_0)(\tau_{p,q}^{(0)}-\tau_{p,q}^{(i)}\}}\sigma_i + \tilde{v}_{n,p,q} \tag{29}$$

$\tilde{v}_{n,p,q}$ is the noise after compensation. Then,

$$\tau_{p,q}^{(0)} - \tau_{p,q}^{(i)} = \frac{\|o - Z_p\| + \|W_q - o\| - \|h_i - Z_p\| - \|W_q - h_i\|}{C} \tag{30}$$

With,
Z_p the p-th transmitter et W_q the q-th receiver.

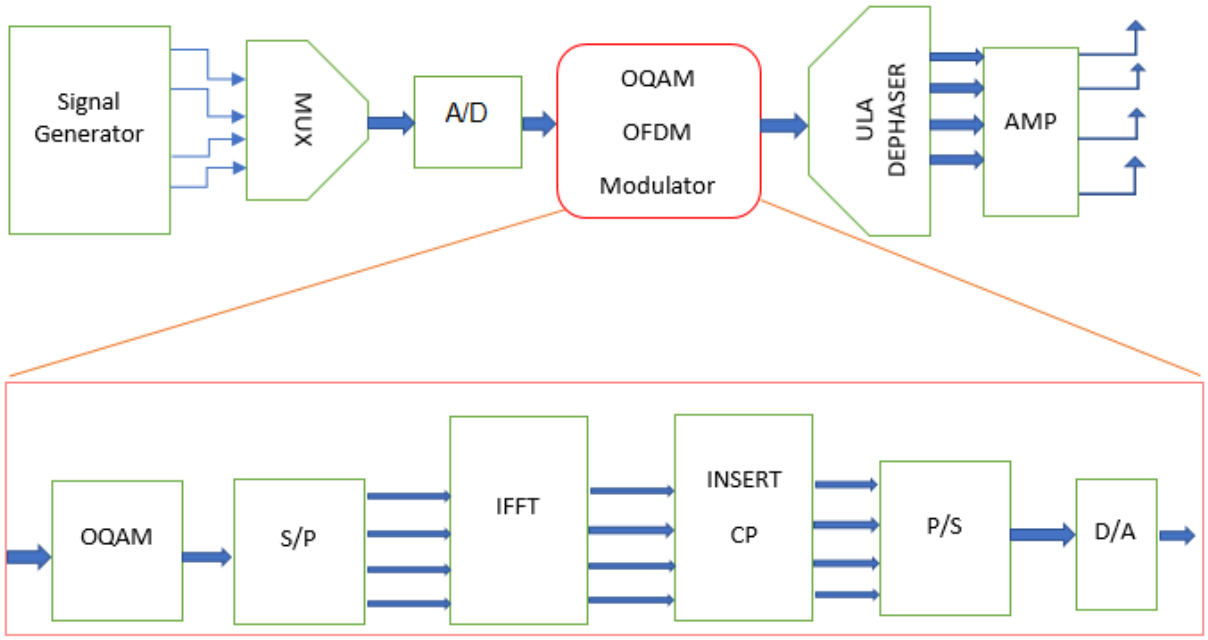

Figure no 4: OFDM OQAM transmitter for MIMO Radar

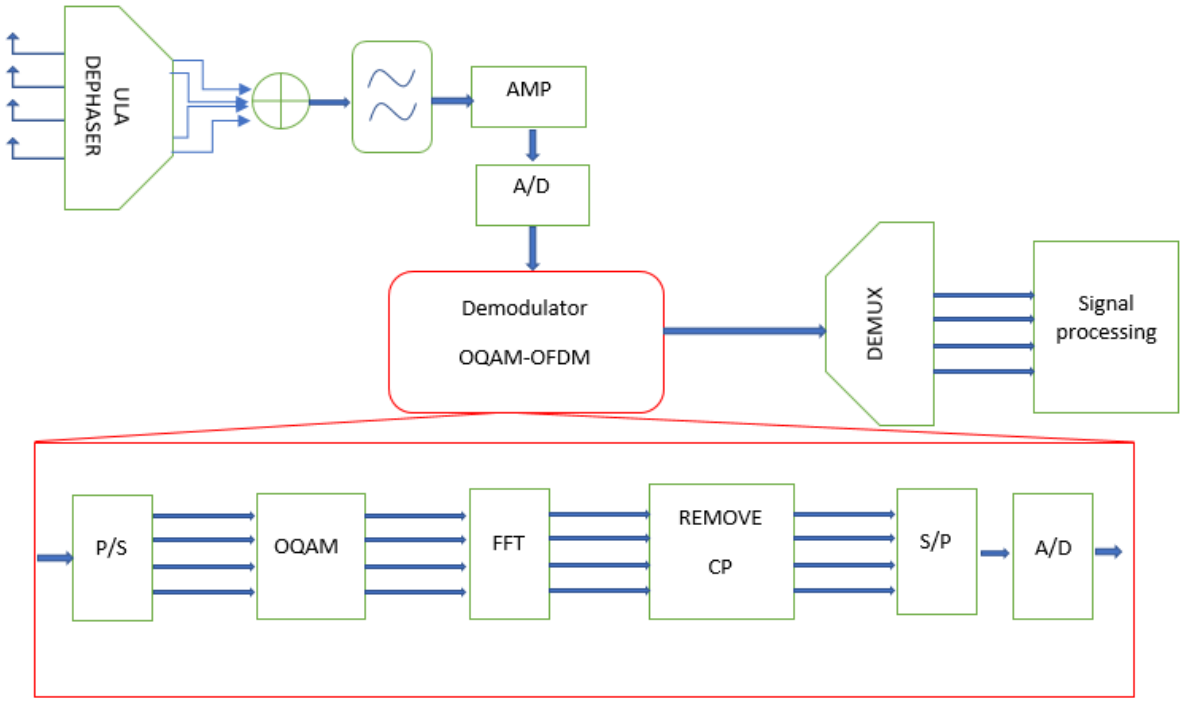

Figure no 5: OFDM OQAM receiver for MIMO Radar

The operators in the figure no 4 and figure no 5 are :

- Signal generator : generate binary data to be sent
- MUX : Multiplexing the multiple signals generated to be sent on one channel
- A/D : Analog to digital
- S/P : Serial to Parallel
- IFFT : Inverse Fast Fourier Transform
- CP : Clipping
- ULA dehaser : equation (10)
- AMP : Amplifier
- D/A : Digital to Analog
- P/S : Parallel to Serial
- FFT : Fast Fourier Transform

If $\tilde{\sigma}_i = \sigma_i \exp\{j2\pi \frac{(-2u_i+\mu_i)}{\lambda}\}$ designates the modulated dispersion amplitude phase, which is a constant for a transmitter/receiver chain.

$$\begin{cases} \Delta u = \frac{C}{2N\Delta f} \\ \Delta\tilde{x} = \frac{Cd_0}{Pf_0d_t} \\ \Delta\tilde{y} = \frac{Cd_0}{Qf_0d_r} \end{cases} \tag{31}$$

The equation (31) expresses the resolution of the radial distance and the section respectively, with $\lambda_0 = \frac{C}{f_0}$ being the wavelength of the system. Pd_t and Qd_r is the distances between the transmitters, and QD_r is the distance between the receivers.

$$u_i = \bar{h}_i^T d_0 \tag{32}$$

$$\bar{h}_i = h_i - o \tag{33}$$

$$(\tilde{x}_i, \tilde{y}_i, \tilde{z}_i)^T = \bar{h}_i - u_i d_0 \tag{34}$$

$$\mu_i = \left(\bar{h}_i - u_i d_0\right)^T (Z_0 + W_0) \tag{35}$$

With,
u_i : the radial distance

The signal received is therefore expressed by the equation (36).

$$h_{n,p,q} = \varepsilon_{n,p,q}^{(0)} r_{n,p,q} = \sum_{i=1}^{I} \tilde{\sigma}_i . exp^{\{j\pi\omega_{1,i} + jP\omega_{2,i} + jQ\omega_{3,i}\}} + \tilde{v}_{n,p,q} \tag{36}$$

With, $\begin{cases} \omega_{1,i} = \frac{-2\pi\lambda_i}{N\Delta u} \\ \omega_{2,i} = \frac{2\pi\tilde{x}_i}{P\Delta\tilde{x}} \\ \omega_{3,i} = \frac{2\pi\tilde{y}_i}{Q\Delta\tilde{y}} \end{cases}$

After the OFDM theory on transmitter and receiver signal, the OQAM processing could also be applied to it.

On the OQAM-OFDM, the modulated signal will be expressed by the equation (37).

$$x(t) = \sum_{n=0}^{N-1} \frac{1}{\sqrt{N}} exp^{\left(j2\pi\frac{tn}{N}\right)} s_n = V.S \tag{37}$$

N : Number of subcarriers of IDFT
V : Columns of IDFT
S : vector of symbol O-QAM
s_n : symbol OQAM carried by the n-th subcarrier expressed by the equation (38)

$$s_n(t) = \theta_{l,k} . a_{l,k} . \delta(t - k\frac{T_s}{2}) \tag{38}$$

UFMC-OQAM MIMO RADAR using DFT or FFT
On UFMC, due to the filter with length L and it divided into subband B. The modulated signal using IFFT will be expressed by the equation (39).

$$x(t) = \sum_{i=0}^{B} \sum_{l=0}^{L} \sum_{n=0}^{N-1} \frac{1}{\sqrt{N}} exp^{\left(j2\pi\frac{nt}{N}\right)} s_{i,n}(t) . f(l) \tag{39}$$

Where,
s_n : Symbol carried by the n-th subcarrier
f : Characteristic filter function used on UFMC
N : Number of subcarriers of IDFT
L : length of the filter
B : number of sub-bands

The equation (39) could be simplified using equations with sommation like on equation (40).

$$\underset{[(N+L-1)\times 1]}{x(t)} = \underset{}{\sum_{i=0}^{B}} \underset{[(N+L-1)\times N]}{F_i} \underset{[N\times n_i]}{V_i} \underset{[n_i\times 1]}{S_i} \tag{40}$$

S_i : vector of symbol O-QAM for i-th subband
V_i : Columns of IDFT corresponding to the i-th sub-band
F_i : TOEPLITZ matrix of dimensions which implements signal convolution with filter characteristics.

The matrix form will be expressed by the equation (41) :

$$x = \bar{F}.\bar{V}.\bar{S} \tag{41}$$

Where,
$\bar{F} = [F_1 \ F_2 \ ... \ F_B]$
$\bar{V} = diag\ [V_1 \ V_2 \ ... \ V_B]$
$\bar{F} = [S_1 \ S_2 \ ... \ S_B]^T$

UFMC is like OFDM but it's subdivided into a K susb-band on each IDFT.

To recover the signal, the DFT process should be done as expressed in the equation (42)

$$s_{i,n}(k) = \frac{1}{N}\sum_{k=0}^{N-1} x(k).e^{j\frac{2\pi}{N}k.n} \tag{42}$$

UFMC-OQAM MIMO RADAR using DCT
On UFMC, due to the filter with length L and it divided into subband B. The modulated signal using IDCT will be expressed by the equation (43).

$$x(t) = \sum_{i=0}^{B}\sum_{l=0}^{L}\sum_{n=0}^{N-1} \beta_n.\cos\left(\frac{\pi(2t-1)(n-1)}{2.N}\right)s_{i,n}(t).f(l) \tag{43}$$

Where,
s_n : Symbol carried by the n-th subcarrier
f : Characteristic filter function used on UFMC
N : Number of subcarriers of IDCT
L : length of the filter
B : number of sub-bands

$$\beta_n = \begin{cases} \frac{1}{\sqrt{2}} \ if \ n = 0 \\ 1 \ if \ 2 \le n \le N-1 \end{cases} \tag{44}$$

The equation (43) could be simplified using equations with sommation like on equation (45).

$$\underset{[(N+L-1)\times 1]}{x(t)} = \underset{[(N+L-1)\times N]}{\sum_{i=0}^{B} F_i} \ \underset{[N\times n_i]}{V_i} \ \underset{[n_i\times 1]}{S_i} \tag{45}$$

S_i : vector of symbol O-QAM for i-th subband
V_i : Columns of IDCT corresponding to the i-th sub-band
F_i : TOEPLITZ matrix of dimensions which implements signal convolution with filter characteristics.

The matrix form will be expressed by the equation (46) :

$$x = \bar{F}.\bar{V}.\bar{S} \tag{46}$$

Where,
$\bar{F} = [F_1 \ F_2 \ ... \ F_B]$
$\bar{V} = diag\ [V_1 \ V_2 \ ... \ V_B]$
$\bar{F} = [S_1 \ S_2 \ ... \ S_B]^T$
UFMC is like OFDM but it's subdivided into a K susb-band on each IDCT.

To recover the signal, the DCT process should be done as expressed in the equation (47)

$$s_{i,n}(k) = \sqrt{\frac{2}{N}}.\sum_{k=0}^{N-1} x(k).\beta_k.cos\left(\frac{\pi.(2n-1).(k-1)}{2N}\right) \tag{47}$$

UFMC-OQAM MIMO RADAR using LWT
The ILWT is defined by a sequence $\{Y(z)\}$, and can be given by the equation (48) :

$$y_{ILWT}[t] = \sum_{q=0}^{Q-1}\sum_{n=0}^{N-1}\left(s_{i,n}(t)\right)^q.(2)^{\frac{q}{2}}.\psi\left(2^q.t-n\right) \tag{48}$$

Where,n is the number of sub-carries ($0 \le n \le N-1$), $s_{i,n}(t)$ is the data and $\psi(.)$ denotes the mother wavelets with scaling factor q and shift n for each subcarrier.

On UFMC, due to the filter with length L and it divided into subband B. The modulated signal using ILWT will be expressed by the equation (49).

$$x(t) = \sum_{i=0}^{B} \sum_{l=0}^{L} \sum_{q=0}^{Q-1} \sum_{n=0}^{N-1} (2)^{\frac{q}{2}} . \psi(2^q . t - n) . \left(s_{i,n}(t)\right)^q . f(l) \tag{49}$$

Where,
s_n : Symbol carried by the n-th subcarrier
f : Characteristic filter function used on UFMC
N : Number of subcarriers of ILWT
L : length of the filter
B : number of sub-bands

The equation (49) could be simplified using equations with sommation like on equation (50).

$$\underset{[(N+L-1)\times 1]}{x(t)} = \underset{[(N+L-1)\times N]}{\sum_{i=0}^{B} F_i} \underset{[N\times n_i]}{V_i} \underset{[n_i\times 1]}{S_i} \tag{50}$$

S_i : vector of symbol O-QAM for i-th subband
V_i : Columns of ILWT corresponding to the i-th sub-band
F_i : TOEPLITZ matrix of dimensions which implements signal convolution with filter characteristics.

The matrix form will be expressed by the equation (51) :

$$x = \bar{F} . \bar{V} . \bar{S} \tag{51}$$

Where,
$\bar{F} = [F_1 \ F_2 \ldots \ F_B]$
$\bar{V} = diag\ [V_1 \ V_2 \ldots \ V_B]$
$\bar{F} = [S_1 \ S_2 \ldots \ S_B]^T$

UFMC is like OFDM but it's subdivided into a K susb-band on each ILWT.

To recover the signal, the LWT process should be done as expressed in the equation (52)

$$s_{LWT}^{q}(z) = \sum_{k=0}^{N-1} (x(k)) . 2^{\frac{z}{2}} \psi(2^z . k - q); \quad z = 0,1,2,\ldots,N-1 \ and \ q = 0,1,2,\ldots,N-1 \tag{52}$$

An alternative method for constructing the biorthogonal wavelet transform, the lifting scheme in figure no 6 and figure no 7, has some advantages over the classical standard wavelet transform which are given below.

- It is a spatial domain method,
- It is easy to use for implementation,
- It allows the use of quicker and in-place computations,
- It allows the use of nonlinear, adaptable, disorderedly sampled and integer to integer wavelet transforms,

Another advantage of the lifting scheme is that the LWT and the reverse-LWT shown in figure no 6 and figure no 7 are completely symmetrical to each other. This ensures that LWT can be applied easily.

Filters and subsampling are used in traditional wavelet transform processes. The lifting method was developed by Sweldens in 1992 to reduce the complex mathematical operations used in filtering. The lifting method is the simplest and most efficient method for wavelet transformation.
In the lifting method, the signal is divided into odd and even samples. Instead of filters, Spit Predit and Update processes are applied. Complex calculations are not required for these operations as in traditional methods.

In the figure, U means *Update,* P means *Prediction,* S means *Spit* and M means *Merge*.

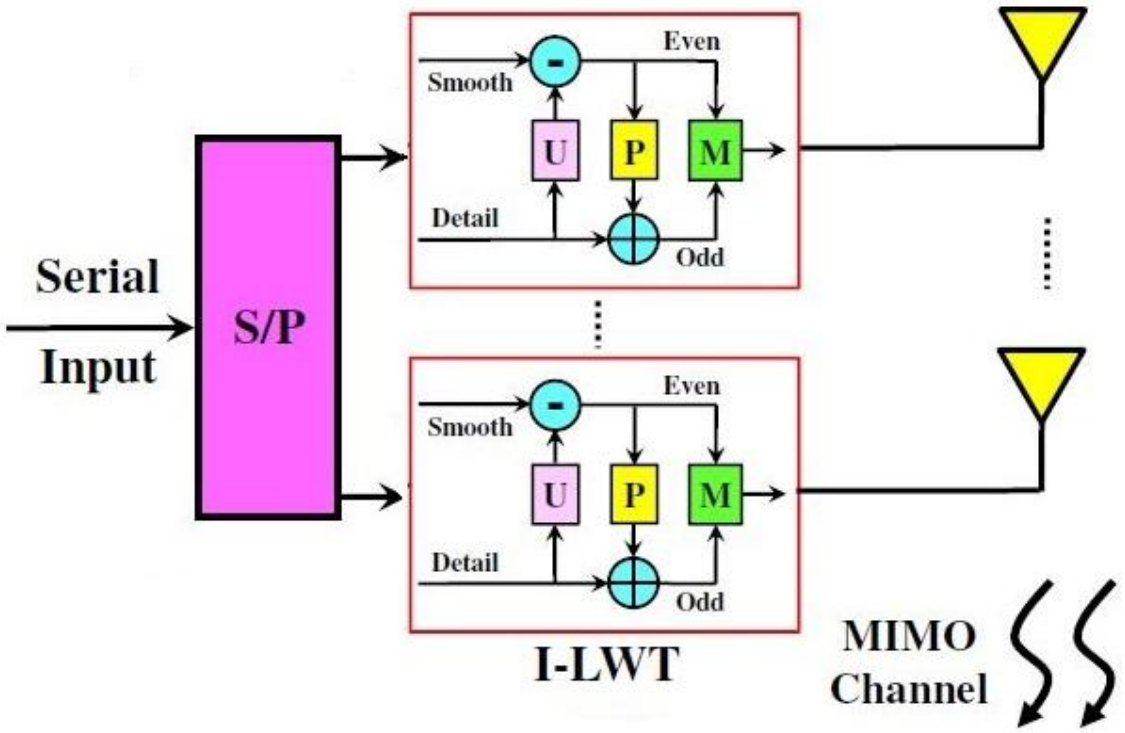

Figure no 6: Fast computation ILWT

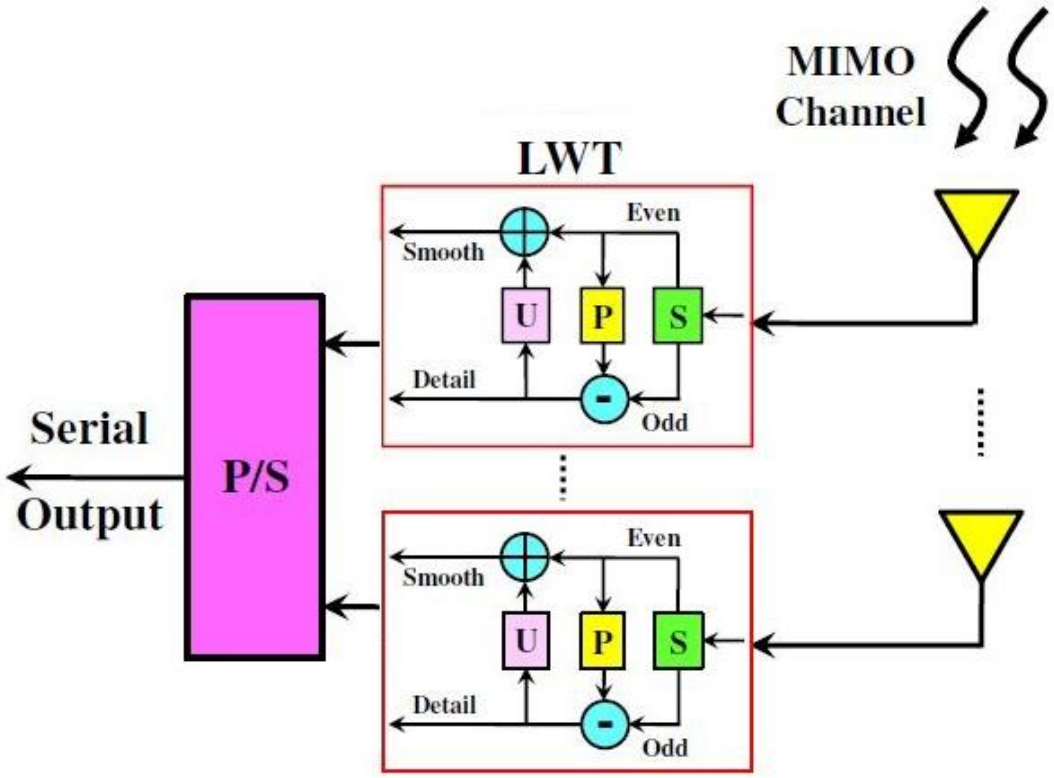

Figure no 7: Fast computation LWT

The original X[k] signal is primarily separated into odd and even components, as in the equations (53) and (54).

$$X_{odd}[k] = X[2k+1] \tag{53}$$

$$X_{even}[k] = X[2k] \tag{54}$$

There is a strong correlation between these two examples. In the predict step, odd samples are tried to be obtained approximately by making use of even samples. The second part, Predict, preserves the high frequency components by eliminating the low frequency components of the signal. In the prediction process, the subset $X_{odd}[k]$ is predicted over the subset $X_{even}[k]$ using the prediction operator P(.). The detail information of the X[k] signal is obtained as in equation (55) by taking the difference between the subset $X_{odd}[k]$ and the predicted P($X_{even}[k]$). The P(.) Prediction operator is a linear combination of a single neighboring subset.

$$P(X_{even}[k]) = \sum_{i} (p_i . X_{even}[k+i]) \tag{55}$$

Here, p_i are the prediction coefficients. This step acts as a high pass filter and the high frequency components (d[k]) that give the detail part of the obtained signal.

$$d[k] = X_{odd}[k] - P(X_{even}[k]) \tag{56}$$

After calculating the prediction p_i,

$$d[k] = d[2y+1] = \begin{cases} X[2y+1] - \dfrac{X[2y] + X[2y+2]}{2} & Normal \\ X[2y+1] - X[2y] & 0dd\ end \end{cases} \tag{57}$$

In the update step, the samples are scaled to fix and then added with even samples to provide low pass filtered values for transformation. In the third part, update, the even components are updated by using the detailed signal to reduce the frequency aliasing effect.

In the update process, the approximate information about the signal is obtained as a result of collecting the detailed information entering the U(.) Update operator with the subset $X_{even}[k]$]. The U(.) Update operator is a linear combination of neighboring d[k] values. The formula for the U(.) Update operator is specified in equation (58).

$$U(d[k]) = \sum_{i} (u_i d[k+i]) \tag{58}$$

Here, u_i are the updating coefficients. In the update process, the approximate value of the obtained signal by passing the signal through a low pass filter is obtained by updating the linear combination of the d[k] prediction difference as in the equation (59). These examples contain low frequency components that give approximate information (s[k])
about the signal.

$$s[k] = X_{even}[k] + U(d[k]) \tag{59}$$

After calculating the prediction u_i,

$$s[k] = s[2y] = \begin{cases} X[2y] + \dfrac{V[2y+1]+1}{2} & Normal \\ X[2y] + \dfrac{X[2y-1] - X[2y] + 1}{2} & Even\ end \end{cases} \tag{60}$$

Inverse transformation is obtained by applying the exact opposite operations used in the conversion to the obtained d[k] and s[k] signals. Inverse Lifting wavelet transformation is given in figure no 6 in I-LWT block in detail.

$$X_{odd}[k] = d[k] + P(X_{even}[k]) \tag{61}$$

$$X_{even}[k] = s[k] - U(d[k]) \tag{62}$$

After the inverse transformation process, as given in equation (63), the original signal is obtained by combining the odd index and even index samples with the MRG combination operator.

$$X[k] = MRG\{X_{odd}[k], X_{even}[k]\} \tag{63}$$

The equations (56) and (59) could be performed using the matrix form expressed in the equation (64).

$$\begin{bmatrix} d[k] \\ s[k] \end{bmatrix} = \begin{bmatrix} 1 & -P(.) \\ U(.) & 1 - P(.)U(.) \end{bmatrix} . \begin{bmatrix} X_{odd}[k] \\ X_{even}[k] \end{bmatrix} = A . \begin{bmatrix} X_{odd}[k] \\ X_{even}[k] \end{bmatrix} \tag{64}$$

With,

$$A = \begin{bmatrix} 1 & -P(.) \\ U(.) & 1 - P(.)U(.) \end{bmatrix} \quad (65)$$

For the ILWT, the equations (61) and (62) could be simplified using the matrix form expressed in the equation (66) :

$$\begin{bmatrix} X_{odd}[k] \\ X_{even}[k] \end{bmatrix} = \begin{bmatrix} 1 - P(.)U(.) & P(.) \\ -U(.) & 1 \end{bmatrix} . \begin{bmatrix} d[k] \\ s[k] \end{bmatrix} = A^{-1} . \begin{bmatrix} d[k] \\ s[k] \end{bmatrix} = A . A . \begin{bmatrix} d[k] \\ s[k] \end{bmatrix} \quad (66)$$

With,

$$A^{-1} = A . A = \begin{bmatrix} 1 - P(.)U(.) & P(.) \\ -U(.) & 1 \end{bmatrix} \quad (67)$$

UFMC-OQAM MIMO RADAR using Inverse Multiple Transforms (IMT) and Multiple Transforms (MT)

In this article, we compare multiple transforms noted Inverve Multiple Transforms (IMT) which uses : IDFT, IDCT and ILWT on the transmitter.

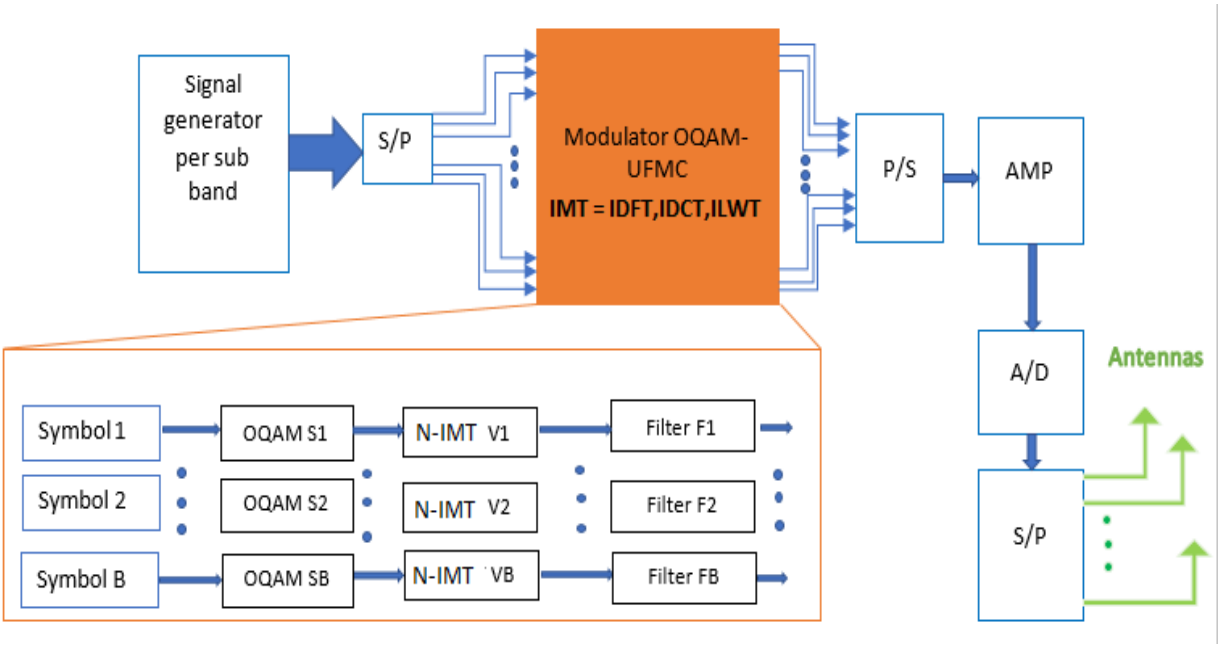

Figure no 8: UFMC OQAM transmitter for MIMO Radar

On the receiver, we use the Multiple Transform (MT) which represents successively by : DFT, DCT and LWT.

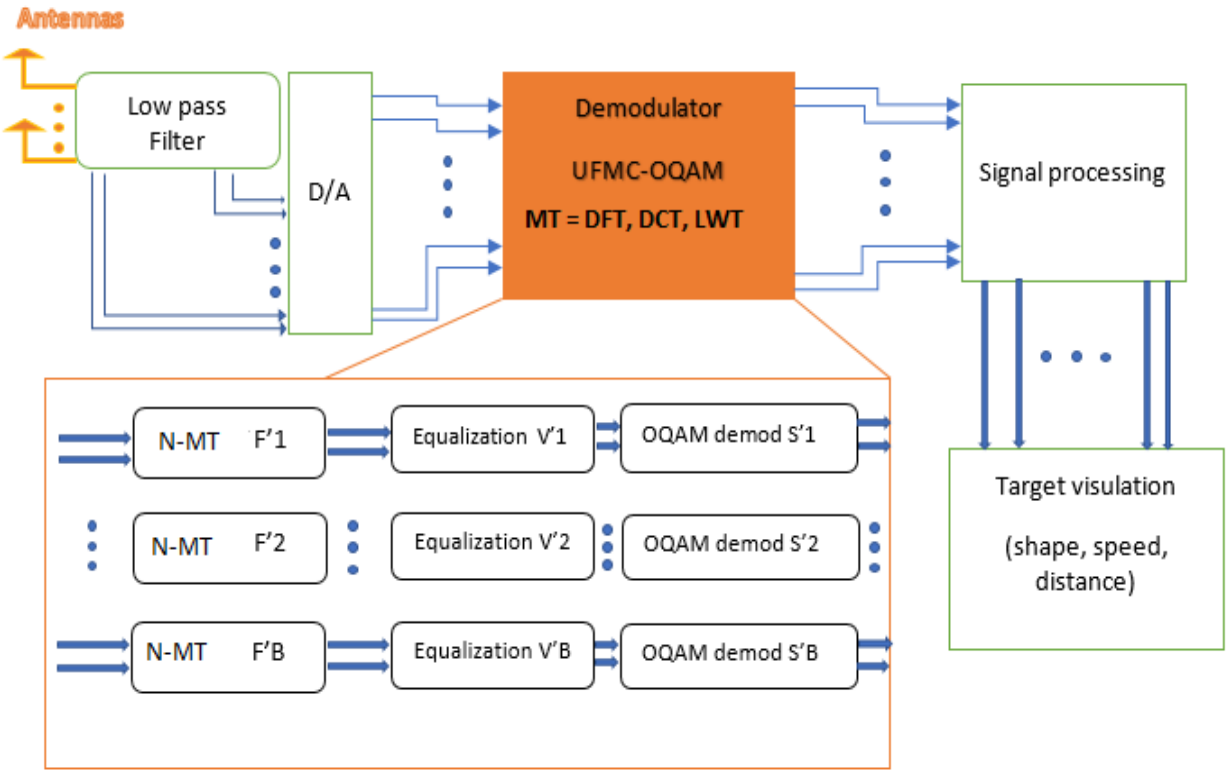

Figure no 9: UFMC OQAM receiver for MIMO Radar

III. Result

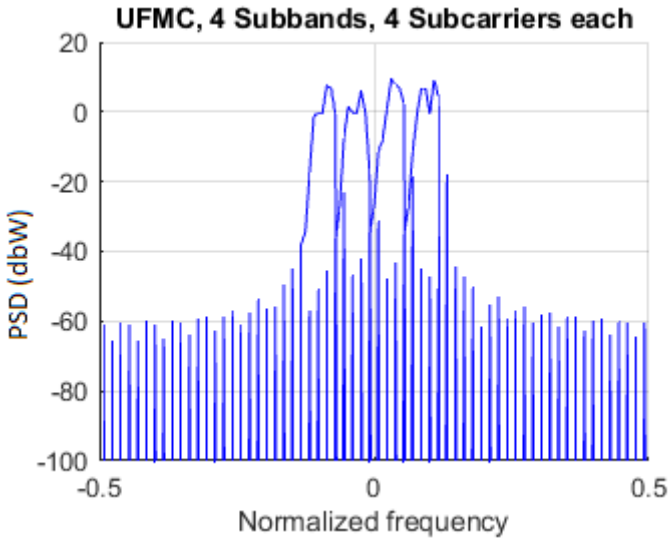

Figure no 10: Power Spectrum density of IDFT-UFMC

After the simulation, all power spectrum density are analyzed using multiple transforms IDFT, IDCT and ILWT like in the figures no 10,11,12.

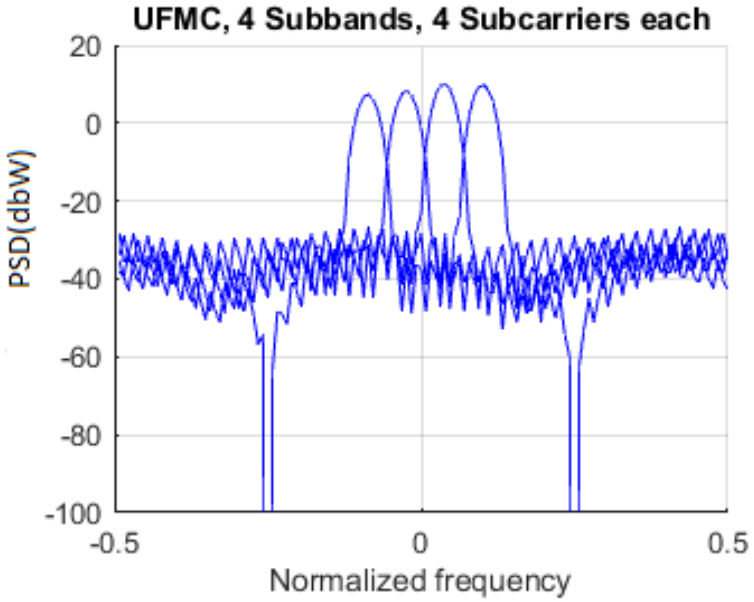

Figure no 11: Power Spectrum density of IDCT-UFMC

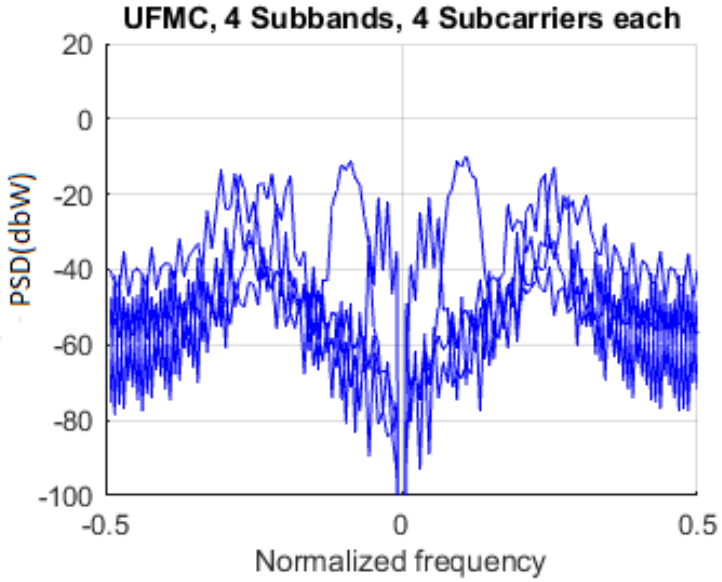

Figure no 12: Power Spectrum density of ILWT-UFMC

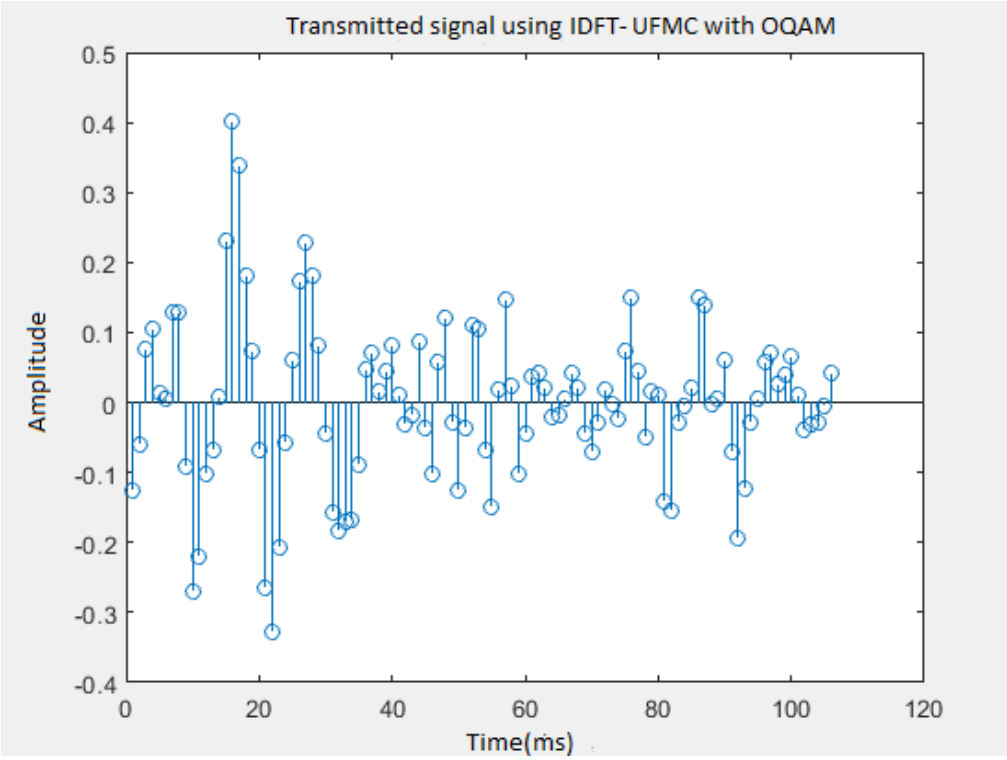

Figure no 13: Modulated signal using IDFT-UFMC with OQAM

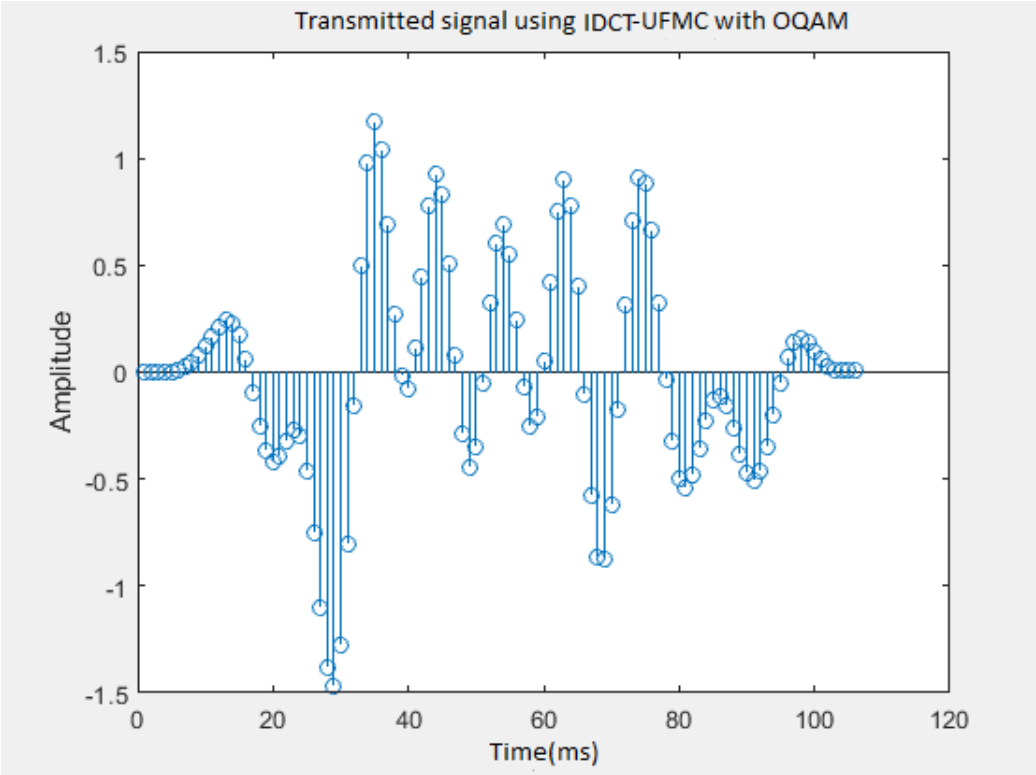

Figure no 14: Modulated signal using IDCT-UFMC with OQAM

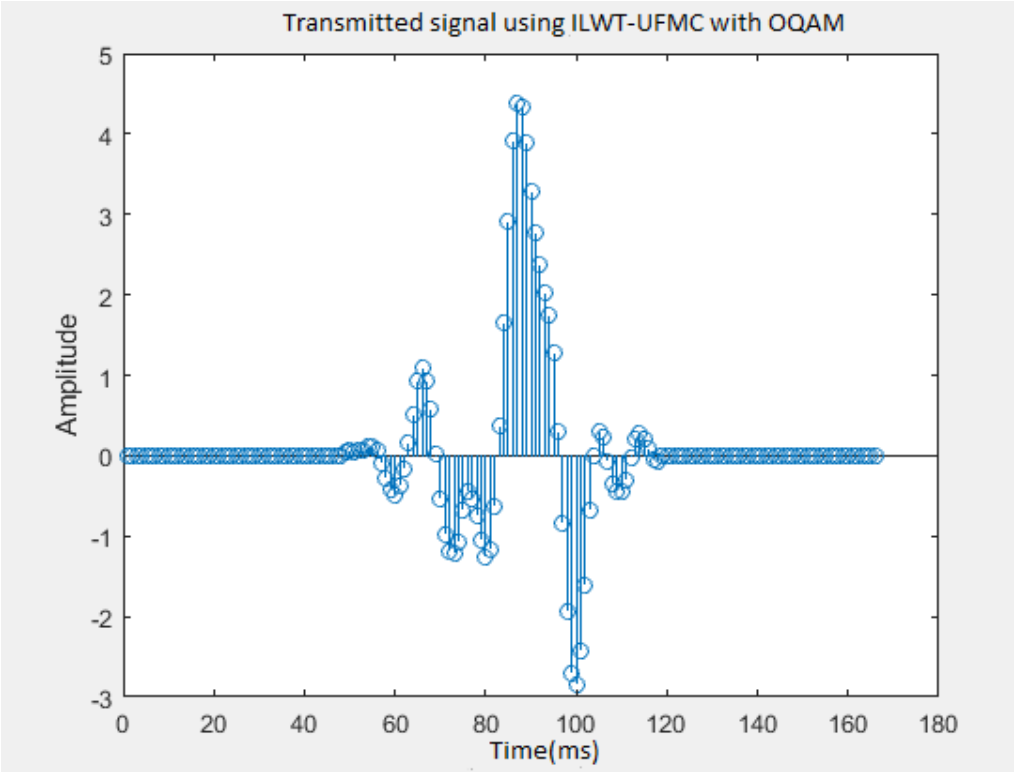

Figure no 15: Modulated signal using ILWT-UFMC with OQAM

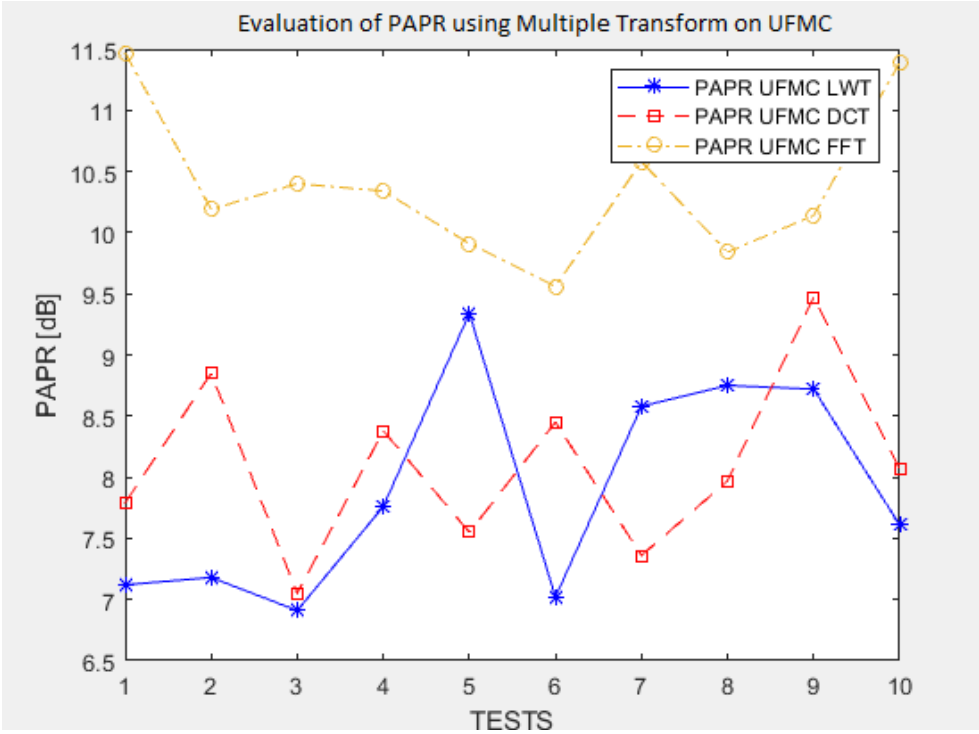

Figure no 16: PAPR Evaluation of UFMC-OQAM with DFT, DCT, LWT

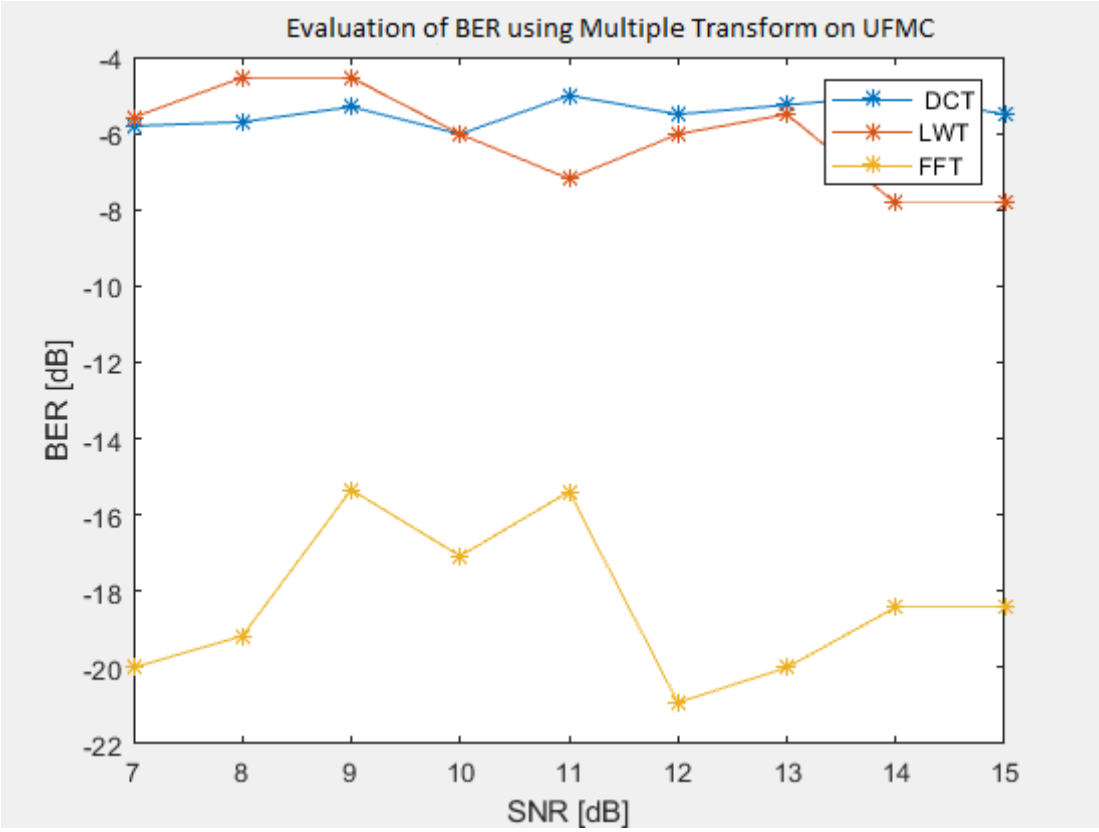

Figure no 16: BER Evaluation of UFMC-OAM with DFT, DCT, LWT

IV. Discussion

Mutli carrier modulation give RADAR MIMO multiple advantages like, doppler effect resistance, reduction of power consumption. This article compares the efficiency of multiple transforms using UFMC modulation with IDFT, IDCT, ILWT.

Following the modulation schema block in figure no 8, and using a spectrum analyzer ; the Power Spectrum Density (PSD) using IDFT is in the figure no 10; using IDCT is in the figure no 11 and using ILWT is in the figure no 12. The simulation has : 4 sub-carries and 4 sub-bands on a UFMC modulator. The first two PSD show that the spectrum is almost the same. It's normal, because IDCT is just a real part of IDFT. The ILWT transform doesn't have more efficiency than the IDFT and IDCT : the in of band of the ILWT is more separated and more not occupied than the two others and the out of band is also bad. I noticed that the ideal spectrum has : in of band maximum and out of band zero. The radar MIMO transmission doesn't need a high data rate, it's not so bad if the in of band is not maximum. The big outside band could interfere with other frequencies and need more efficient filters to prevent it.

Figures no 13, 14, 15 show the modulated signal after the schema bloc of transmitter. The three figures show the inconvenience inconvenient concerning the classic UFMC-IDFT. This modulation has a large variation in the modulated signal instead of the two modulations, UFMC-IDCT and UFMC-ILWT.

The next figure no 16 shows indeed the Peak Average Power Ratio. As a result, the IDFT has a maximum PAPR but the IDCT and ILWT have a minimum PAPR. So, IDCT and ILWT don't consume much power with the amplifier module. Indeed, the ILWT has good power consumption due to this reduction PAPR and also due to the minimum complexity calculation, like in equations (56) (57) and (59) (60) which use linear combination only instead of IDCT, which uses exponential series (infinite calculation using the polynomial infinite interpolation of exponent)

The last figure needs the schema bloc of receiver on figure no 9 and compare the signal sent and signal received. After this, the BER is calculated using the ratio between the error signal and the total signal. The inconvenience of IDCT and ILWT is that it's has a big error ratio instead of IDFT.

This study also shows the advantages of ILWT indeed in power consumption. The ILWT has a quick calculation and a less PAPR, which is a good deal for reduction of power consumption. That's why ILWT is proposed on 6G transmission. The IDCT is the second choice and IDFT is the last choice . But, the ILWT doesn't have a good power spectrum and BER evaluation. Using a code corrector of error could be a good solution in this problem.

V. Conclusion

As conclusion, UFMC-ILWT gives a good power consumption with MIMO-RADAR. The wavelet transform is very quick and has a less PAPR. The UFMC-IDCT is the second choice but it's not have a quick time processing. For having high data rate, the UFMC-ILWT should use a good code corrector error to resolve the problem about Bit Error Ratio (BER). This proposition is not so useful on RADAR MIMO due less data rate transmitted on it.

References

[1]. Zhou, Zhenlei, Lin, Bangjiang, Tang, Xuan, Chaudhary, Sushank, Lin, Chun, "Performance comparison of DFT-OFDM, DCT-OFDM, and DWT-OFDM for visible light communications", spie. Journal, International Conference on Optical Communications and Networks, 2018, Zuhai China.

[2]. Javaid A. Sheikh, Farhana Mustafa, Arshid Iqbal "Resource Allocation of Power in FBMC based 5G Networks using Fuzzy Rule Base System and Wavelet Transform", International Journal of Advanced Research in Science and Engineering (IJARSE), march 2018.

[3]. Zainab Hdeib Al-Shably, Zahir M. Hussain, "Performance of FFT-OFDM versus DWT-OFDM under Compressive Sensing", Journal of Physics: Conference Series, 2021

[4]. Khaizuran Abdullah, Zahir M. Hussain, "Studies on DWT-OFDM and FFT-OFDM Systems", International Conference on Communication, Computer and Power (ICCCP 2009)

[5]. Elif Büşra Tuna, Yusuf İslam Tek, Ali Ozen, "A Novel Approach based on Lifting Wavelet Transform for MIMO-OFDM Systems", Research square 2021

[6]. Sheela M. S., Sukera T. P., Arjun K. R., "Comparaison of FFT-OFDM and DWT-OFDM System in Digital Communication", International Journal of Engineering Research and Technology, IJERT 2018

[7]. Meryem Maras, Elif Nur Ayvaz, Meltem Gömeç, Asuman Sava¸scıhabes, Ali Özen, "A Novel GFDM Waveform Design Based on Cascaded WHT-LWT Transform for the Beyond 5G Wireless Communications", MDPI 2021

[8]. Shanlin wei, Hui li, Wenjie Zhang, Wei Cheng, "A comprehensive performance evaluation of Universal Filtered Mutli-Carrier Technique"

[9]. Zahraa Abdel Hamid, Fathl E. Abd El Samie, "FFT/DWT/DCT OFDM channel estimation using EM algorithm in the presence of chaotic interleaving", IEEE 2012

[10]. Mitali Sahu, Meha Shrivastava, Abhishek Agwekar, "Review of PAPR reduction for MIMO-OFDM Radar with DWT and DCT Multiple Contrainsts", International Journal of Engineering Research and Technology, IJERT 2019.

[11]. B.Prasanna Lakshmi, K.Govinda Rajulu, "DWT based barcode modulation for efficient and secure data transmission through DPSK-OFDM"International Research Journal of Engineering and Technology, IRJET, 2017

[12]. Enggar Fransiska DW, Octarina Nur Samijayan, J Suci Rahmatia, "Design and Performance Investigation of Discrete Wavelet Transform (DWT) Based OFDM using 4-PAM for Indoor VLC System", International Conference on Information and Communication Technology, ICoICT 2019

[13]. Ch.Gangadhar, Md. Habibulla, "Spectral Efficiency Enhancement Through Wavelet Transform Filter Bank for Future Mobile Communications", International Journal of Innovative Technology and Exploring Engineering, IJITEE 2019

[14]. Elif Nur Ayvaz, Meryem Maras, Meltem G¨omec, Asuman Savas¸cıhabes, Ali Ozen, "A Novel Concatenated LWT and WHT Based UFMC Waveform Design for the Next Generation Wireless Communication Systems" IEEJ TRANSACTIONS ON ELECTRICAL AND ELECTRONIC ENGINEERING, 2021

[15]. Engin ÖKSÜZ, Ahmet ALTUN, Büşra ÜLGERLİ, Gökay YÜCEL, Ali ÖZEN, "A Comparative Performance Analyses of FFT Based OFDM and DWT Based OFDM Systems", journal of new result in science, JNRS 2016

[16]. Simmi Garg, Anuj Kumar Sharma, Anand Kumar Tyagi, "Performance Comparison of Proposed Scheme Coded DWT-OFDM System with that of Conventional OFDM", Journal of Unversity of Shanghai for Science and Technology, 2020

[17]. Manjunatha K, Reshma M, "Comparative Study on DWT-OFDM and FFT-OFDM Simulation Using Matlab Simulink", International Journal of Engineering Trends and Technology, IJETT, 2017

[18]. Wim Sweldens, "The Lifting Scheme: A New Philosophy in Biorthogonal Wavelet Constructions", Department of Computer Science

Marie Emile RANDRIANANDRASANA, et. al. "Power consumption reduction on RADAR MIMO using Lift Wavelet Transform – Universal Filtered Multicarrier (LWT-UFMC)." *IOSR Journal of Computer Engineering (IOSR-JCE)*, 24(2), 2022, pp. 39-59.